J Mater Sci: Mater Med (2010) 21:2601–2609
DOI 10.1007/s10856-010-4123-4

Effect of strontium ions substitution on gene delivery related properties of calcium phosphate nanoparticles

A. Hanifi · M. H. Fathi · H. Mir Mohammad Sadeghi

Received: 8 April 2010 / Accepted: 29 June 2010 / Published online: 10 July 2010

Abstract Gene therapy has been considered a strategy for delivery of therapeutic nucleic acids to a specific site. Calcium phosphates are one gene delivery vector group of interest. However, low transfection efficiency has limited the use of calcium phosphate in gene delivery applications. Present work aims at studying the fabrication of strontium substituted calcium phosphate nanoparticles with improved gene delivery related properties. Strontium substituted calcium phosphate was prepared using a simple sol gel method. X-ray diffraction analysis, Fourier transform infrared spectroscopy, transmission electron microscopy, specific surface area analysis, zeta potential measurement and ion release evaluation were used to characterize the samples. This characterization showed strontium and carbonate co-substituted calcium phosphate which resulted in nano size particles with low crystallinity, high specific surface area, positive surface charge, and a high dissolution rate. These improved properties could increase the DNA concentration on the vector as well as the endosomal escape of the complex that leads to higher transfection efficiency of this novel gene delivery vector.

A. Hanifi (✉) · M. H. Fathi
Biomaterials Group, Materials Engineering Department, Isfahan University of Technology, Isfahan 84156-83111, Iran
e-mail: a.hanifi@gmail.com

H. Mir Mohammad Sadeghi
Biotechnology Department, Faculty of Pharmacy and Pharmaceutical Sciences, Isfahan University of Medical Sciences, Isfahan, Iran

1 Introduction

Gene therapy has been considered a strategy for the delivery of therapeutic genes to a tissue site [1]. Several non viral and viral vectors are available for gene delivery. An ideal vector will have a high transfection efficiency, low toxicity, and consistent gene expression [2].

Among non viral gene delivery vectors, calcium phosphate (CaP) mediated transfection of mammalian cells with DNA has been a useful approach to enhance DNA transfection efficiency. DNA-calcium phosphate complex has been used for in vitro transfection since the 1970s due to its good biological characterization [3].

Efficient gene transfection is achieved when the gene delivery vector effectively facilitates the DNA condensation on the vector, the physical and chemical stability of the DNA in the extracellular matrix, cellular uptake, endosomal escape, cytosolic transport, and nuclear localization of the DNA for transcription [4].

In the case of calcium phosphate based approaches, compared to viral approaches, lower levels of gene expression are observed. This is due to difficulties associated with low amounts of DNA condensation on the vector and endosomal escape of the complex [4].

As the gene delivery properties of the calcium phosphate nanoparticles are related to the crystal-size, crystallinity and composition, changes in the chemical composition of nanoparticles, using ionic substitution, could improve these properties [5, 6]. The physico-chemical properties of calcium phosphate particles can be improved by substitution with ions usually present in natural bone, i.e., cations (Mg^{2+}, Zn^{2+}, Mn^{2+}, Na^{+}, Sr^{2+}) and anions (CO_3^{2-}, F^{-}, HPO_4^{2-}) [7].

In recent years, the incorporation of strontium (Sr) into the calcium phosphate structure due to its presence in

calcified bone has been witnessed [8]. The first work done on the effect of Sr substitution in apatite structure was completed in the 1960s [9]. Since that time, a number of reports have been published on this issue [10–13]. Strontium changes the crystallinity and dissolution rate of the calcium phosphate as well as the net positive charge of calcium phosphate nanoparticles [10–13]. Improving these properties could be effective in gene delivery efficiency of the calcium phosphate vectors.

Isotherm analysis reveals that, electrostatic forces are the main driving force of DNA binding to calcium phosphate [14]. Nucleic acids bind to calcium phosphate through the interaction of cations on calcium phosphate and the phosphate groups of nucleic acids [15]. Therefore, increasing the net positive charge and cationic strength of the calcium phosphate vector using Sr substitution leads to enhanced DNA condensation on the vector. This appears to improve gene delivery efficiency of the DNA-calcium phosphate complex.

Furthermore, increasing the chance of the endosomal escape of the complex could significantly affect the gene delivery efficiency of the system. One promising strategy to release internalized complexes from the endosome is the "Proton sponge hypothesis", discussed in 1995 by Boussif et al. [16, 17]. Proton sponge hypothesis assumes H^+ and Cl^- entry into the endosome which leads to osmotic swelling, and rupture of endosome, resulting in the release of the vector into the cytoplasm.

According to the literature [11, 12, 18, 19], substitution of Sr^{2+} ions into the calcium phosphate structure increases the dissolution rate of nanoparticles in physiological medium. This results in higher concentration of Ca^{2+} and Sr^{2+} inside the endosome. It has been demonstrated that calcium ions play an important role in endosomal escape, through the proton sponge mechanism [20]. Cations like calcium and strontium increase the proton uptake of the endosome compartment and cause it to rupture, introducing a higher fraction of delivered gene to the cytoplasm.

Considering the therapeutic properties, strontium has a beneficial effect on bone [21]. Sr is present in the mineral phase of bone, especially at the regions of high metabolic turn-over [22]. In vitro and in vivo studies have indicated that orally administered strontium increases bone formation, the number of bone forming sites, bone mineral density, and reduces bone resorption [11]. In addition, stimulatory effects on bone collagen synthesis in cell cultures have been specifically correlated to Sr [23].

In line with its chemical analogy to calcium, Sr is a bone seeking element [5]. The presence of Ca and Sr ions in calcium phosphate nanoparticles can lead to targeted delivery of the vector to bone sites.

Keeping this viewpoint, Sr substitution in the calcium phosphate structure would be helpful for increasing bone generation as well as targeting the non viral vector to the specific bone tissue.

Accordingly, the aim of this work was to study the effect of Sr substitution on physical properties of calcium phosphate nanoparticles. Sr substitution in the calcium phosphate structure may change the crystallinity, specific surface area, net positive charge, and chemical composition of the resultant nanoparticles. These characteristics would serve to increase the fraction of genetic material that both successfully condensed on the calcium phosphate vecto, and escaped the endosomal compartment, improving transfection efficiencies.

Sr substituted calcium phosphate powders have been prepared by ion exchange of Sr^{2+} for Ca^{2+} using a biomimetic approach [24], wet chemical synthesis [25, 26], and solid-state route [10]. This study attempted to prepare Sr substituted calcium phosphate through a simple sol gel method.

2 Experimental

2.1 Sample preparation

Calcium phosphate nanoparticles containing Sr^{2+} ions were synthesized via a simple sol–gel method [27]. Briefly, phosphoric pentoxide (P_2O_5, Aldrich), calcium nitrate tetrahydrate ($Ca(NO_3)_2{\cdot}4H_2O$, Aldrich) and strontium nitrate ($Sr(NO_3)_2$, Aldrich) were used to prepare precursors. Designated amounts of Ca-precursor and P-precursor were mixed to form the CaP mixture. Sr-precursor was added drop-wise into Ca–P mixture to obtain a solution with (Ca + Sr)/P ratio of 1.67. Strontium substituted calcium phosphate samples were prepared in five different concentrations of Sr^{2+} ions in apatite lattice as described in Table 1.

The suspension of the reaction product was maintained under stirring for 3 h at room temperature to form a gel. The final gel was aged for 24 h at room temperature, washed, filtered, dried overnight at 80°C, and then calcinated at a temperature of 600°C in air. Calcination temperature and aging time were chosen based on the previous study [27, 28].

The atomic concentrations of elements (Ca, P and Sr) in the final samples were quantified by X-ray fluorescence spectroscopy (XRF using JEOL JSX-3201Z Element Analyzer) to compare with a prepared concentration and stoichiometric ratio of Ca, P and Sr. Results are summarized in Table 1.

It has been proven that this simple sol–gel method is a self controlling process [27], thus no additional chemicals (i.e., ammonia) are needed to adjust the pH of the solution.

Table 1 Composition of prepared strontium substituted calcium phosphate samples

Sample name	Sample composition		(Ca + Sr)/P ratio		Calcination temp. (°C)
	As prepared	XRF	As prepared	XRF	
0.0Sr-CaP	0.00	0.03	1.67	1.70	600
0.5Sr-CaP	0.50	0.56	1.67	1.68	600
1.0 Sr-CaP	1.00	1.04	1.67	1.72	600
5.0 Sr-CaP	5.00	5.18	1.67	1.63	600
10.0Sr-CaP	10.00	10.26	1.67	1.74	600

2.2 Phase composition evaluation

The chemical composition of calcium phosphate nanoparticles was evaluated by X-ray diffraction (XRD, Philips X'Pert PRO, USA). The diffraction spectra were recorded in the 2θ range from 20°–70° using Cu-Kα (wavelength = 1.54056 Å, 40 mA, 40 kV) radiation with a step size of 0.05° and a step duration of 1 s.

The volume fraction of the beta-tricalcium phosphate phase was calculated using Chung et al. method [29]. According to Chung's method the amount of β-TCP in the final product has an indirect relationship with the I_{217} TCP / I_{211} HA ratio, where I_{217} TCP is the relation intensity of the (217) crystallographic planes of the TCP, and I_{211} HA is the relation intensity of the (211) crystallographic planes of the HA in the XRD patterns.

2.3 Crystal size and crystallinity measurement

Based on Scherrer's equation [30] a single-crystal dimension perpendicular to the (hkl) plane can be estimated from the peak broadening as:

$$D_{hkl} = k\lambda / B_{1/2} \cos\theta_{hkl} \quad (1)$$

where D_{hkl} (nm) is single crystal size; k is a constant varying with the method of measuring and is chosen to be 0.9; λ is the wavelength (nm) of Cu Kα radiation ($\lambda = 0.15418$ nm); $B_{1/2}$ corresponds to full width at half maximum (FWHM) for the hkl peak (rad); and θ_{hkl} is the diffraction angle (in degrees).

For Sr substituted calcium phosphate samples the line broadening of the (002) reflection was used to evaluate the crystal size.

The crystallinity degree of samples (Xc) corresponding to the fraction of the crystalline phase present in the examined volume was evaluated by the relation [31]:

$$Xc \approx 1 - V_{112/300} / I_{300} \quad (2)$$

where I_{300} is the intensity of (300) reflection of HA and $V_{112/300}$ is the intensity of the hollow between (112) and (300) reflections. In agreement with Landi et al. this was verified with the relation [32]:

$$Xc = \left(K / B_{1/2}\right)^3 \quad (3)$$

where K is a constant set at 0.24 and $B_{1/2}$ is the FWHM of the (0 0 2) reflection (in degrees).

2.4 Particle size analysis

Transmission electron microscopy (TEM, Philips CM30, USA) was utilized for evaluation of the particle size. TEM samples were prepared using an ultrasound vibration method [33]. The samples were immersed in ethanol solution and subjected to ultrasound vibration for 15 min to disperse the precipitate powder homogeneously. Then, the precipitates were carefully extracted from the suspension of the sample and picked up using TEM copper meshes with carbon film coatings. After drying under ambient conditions, the samples on the copper meshes were examined by TEM.

2.5 Infrared spectroscopy

Infrared spectroscopy was used to identify different functional groups in apatite structure. Using Fourier transform infrared spectroscopy (FTIR, PerkinElmer, USA), the spectrum was recorded in the 4000–400 cm^{-1} region with 2 cm^{-1} resolution.

2.6 Specific surface area measurement

The specific surface area (SSA) of the nanoparticles was evaluated by the Brunauer–Emmett–Teller (BET) method using Micromeritics Device (Norcross, USA). Sample outgassing was performed at 100°C for 24 hours before the analysis. The particle size (d_{BET}) was also estimated assuming the primary particles were spherical [32];

$$d_{BET} = 6 / \rho \cdot s \quad (4)$$

where ρ is the theoretical density of the sample (3.156 g/cm^3) and s is the specific surface area.

2.7 Zeta potential measurement

The surface charge of Sr substituted calcium phosphate nanoparticles was determined by measuring the zeta

potential in the physiologic pH range. Zeta potential was measured with a Zetasizer Nano-ZS (Malvern Instruments Ltd., UK) and values were expressed as a mean ± standard deviation of three measurements.

2.8 Ion dissolution rate measurements in simulated body fluid

The solubility of calcium phosphate nanoparticles determines the amount of calcium and strontium ions released. This is important for increasing endosomal escape efficiency of the gene delivery systems. Two parameters substantially influence the solubility of calcium phosphate at physiological conditions: the crystallinity grade of the powders and the addition of substituted groups in the apatite. In order to compare the dissolution rate of the Sr substituted samples with normal calcium phosphate, simulated body fluid (SBF) was used to evaluate Ca^{2+} and Sr^{2+} release from Sr substituted calcium phosphate nanoparticles.

An ion release test was performed in a SBF medium of pH 7.4 at a ratio of 1 mg/ml in a water bath at 37 °C. The SBF medium consists of 9 g NaCl, 5 g KCl and 0.2 g $MgHPO_4 \cdot 3H_2O$ per liter [34]. The amount of cations in the SBF medium was determined by an atomic absorption spectrometer (AAS, PerkinElmer, USA).

3 Results and discussion

3.1 Phase composition, crystal size and crystallinity

Figure 1 shows the X-ray diffraction patterns of Sr substituted calcium phosphate samples with different amounts of strontium. XRD patterns of the samples detected a broad peak for (002) planes which are typical for nanocrystalline apatite [27].

The apatite hexagonal cell parameters were measured as a = b = 9.312 Å and c = 6.941 Å for Sr substituted calcium phosphate. These values are greater when compared with the stoichiometric HA parameters as a = b = 9.418 Å and c = 6.885 Å, proving that Sr has been incorporated in the apatite structure.

Furthermore, XRD peaks deviated from the standard HA peaks with an increase of strontium concentration. This could be due to the incorporated strontium ions. Since the ionic radius of Sr^{2+} (1.13Å) is higher than that of the Ca^{2+} (0.99Å).

Considering the position of the Sr^{2+} ions in apatite structure, the preferred distribution of Sr^{2+} ions at the five crystallographic independent Ca-sites of apatite structure has been confirmed by Kannan et al. [10]. The favorable insertion of Sr^{2+} in the Ca(4) sites is also supported by the work of Renaudin et al. [35]. Their work has confirmed the stabilizing effect of Sr in the Ca(4) site.

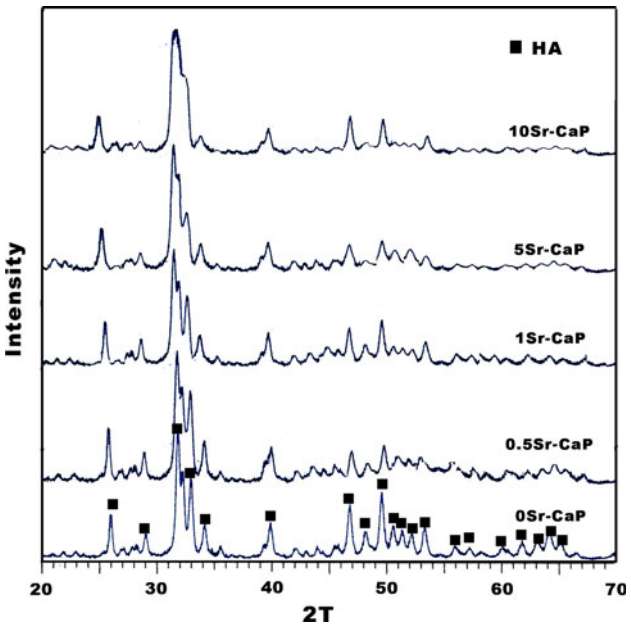

Fig. 1 XRD patterns of Sr substituted samples with different amount of substituted ions

Crystal size values of different samples are presented in Table 2. Increasing the amount of strontium ion substitution in apatite structure has resulted in smaller size particles.

Furthermore, the effect Sr^{2+} on peak broadening, and crystal size of the particles is higher for Sr values above 1% in this study. Sr incorporation at 1% and less did not significantly change the patterns of Sr substituted calcium phosphate. Li et al. has reported a similar effect for Sr values more than 1.5% for Sr substituted calcium phosphate nanoparticles [5].

A reduction in Sr substituted calcium phosphate crystal size at different Sr concentrations was previously reported by Christoffersen et al. [19].

However, it is shown that the crystallinity of apatite decreased with the increase of strontium content (Table 2).

With the incorporation of Sr in apatite crystal, the distance of Sr-hydroxyl will be greater than that of Ca-hydroxyl [5]. Consequently, decreases in lattice energy and crystallinity are possible. This result corroborates the decrease of crystallinity induced by Sr substitution verified by several studies [5, 18, 36].

Strontium substitution in calcium phosphate nanoparticles has no significant effect on phase composition and the stability of the beta-tricalcium phosphate phase. Therefore, it seems that strontium could not be considered as a β-TCP stabilizer in the calcium phosphate structure.

From X-ray diffraction patterns of the samples, it can be concluded that the Sr incorporation in calcium phosphate

Table 2 Crystal size, crystallinity and phase composition of the samples

Sample	Sample composition	Peak width (rad)	Crystal size (nm)	Crystallinity (Xc) (%)	HA/β-TCP (%)
1	0.0Sr-CaP	0.0042	33.4 ± 3	64	97/3
2	0.5Sr-CaP	0.0045	31.2 ± 2	60	94/6
3	1.0 Sr-CaP	0.0050	28.3 ± 1	58	93/7
4	5.0 Sr-CaP	0.0072	19.7 ± 1	51	89/11
5	10.0Sr-CaP	0.0078	18.1 ± 2	49	87/13

crystal may lead to modifications in lattice parameters, crystal size, and the crystallinity of nanoparticles. Decreasing the size of the particles results in higher surface area of the calcium phosphate vector and could increase the concentration of DNA on the vector. In addition, lower crystallinity of Sr substituted nanoparticles enhances the solubility of the vector in physiological medium which increases the chance of endosomal escape of the gene delivery complex.

3.2 Particle size analysis

The transmission electron microscopy (TEM) images confirm the X-Ray diffraction (XRD) data, that the presence of strontium ions in apatite structure decreases the particle size (Fig. 2).

Some similar results were previously reported on decreasing the particle size of Sr substituted calcium phosphate for high amounts of Sr ions above 1.5% [5, 25]. Although the XRD and TEM results of the present study indicated that below 1%, strontium did not change the crystal size significantly, the trend of decreasing of the particle size is consistent for all values of Sr concentration.

As a conclusion of XRD and TEM analysis, the changes in crystal size and crystallinity of Sr substituted calcium phosphate could be due to the Sr^{2+} substitution of Ca^{2+} [10, 11, 36]. Smaller nano size particle of the Sr substituted calcium phosphate could enhance the DNA binding on calcium phosphate based vectors. This will eventually result in improved gene delivery process.

3.3 Infrared spectroscopy

FTIR spectra of Sr substituted calcium phosphate nanoparticles are shown in Fig. 3. The absorption bands of phosphate group detected at 960–1100 cm^{-1} and 560–600 cm^{-1}

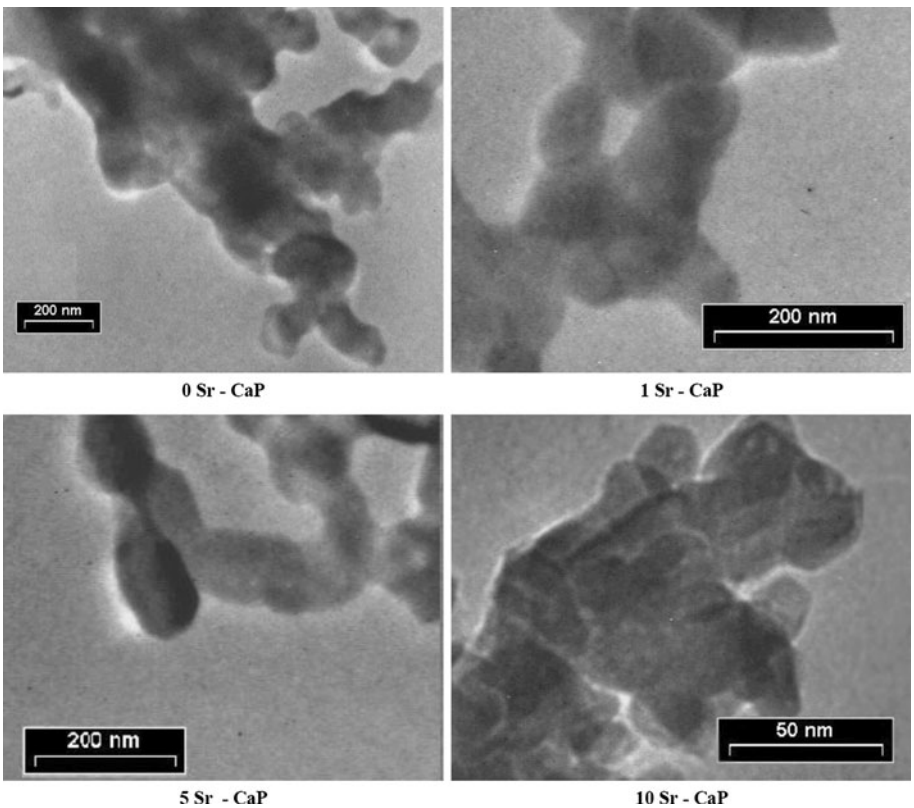

Fig. 2 TEM micrograph of Sr substituted calcium phosphate nanoparticles with different amount of strontium

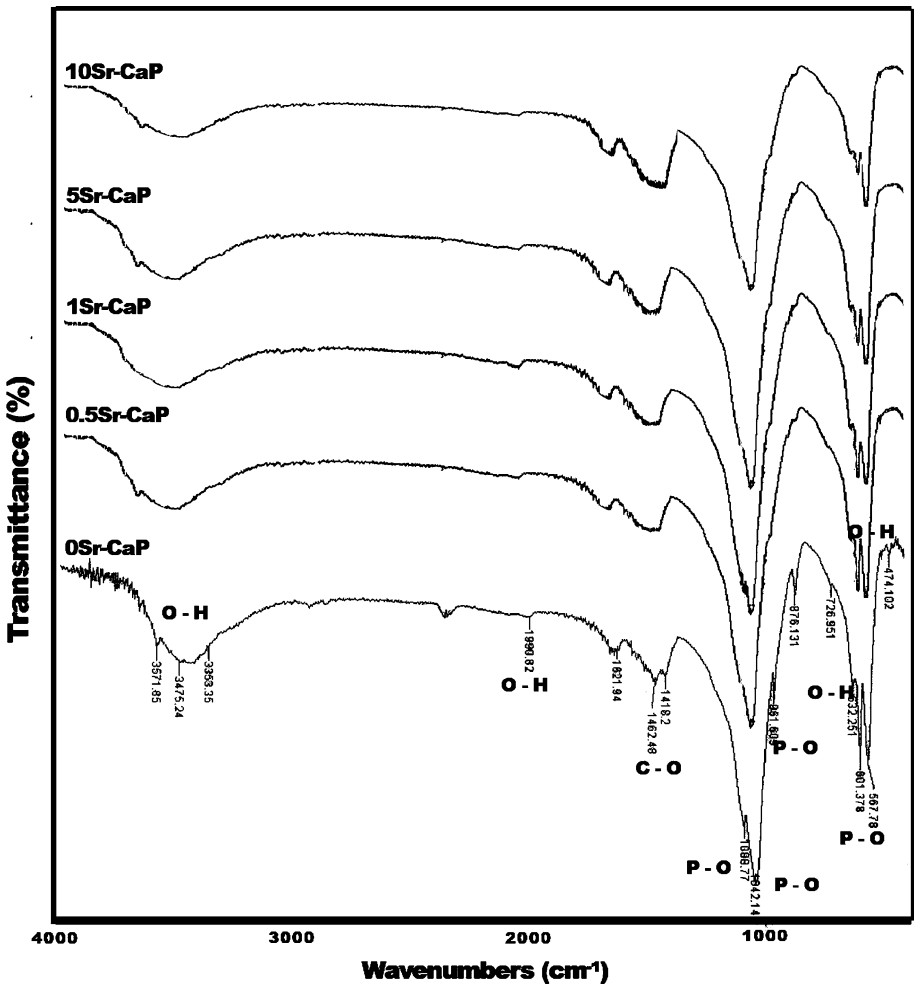

Fig. 3 FTIR spectra of Sr substituted calcium phosphate nanoparticles with different amount of strontium

are the characteristic peaks which are presented in all FTIR spectra of calcium phosphate samples [34, 37, 38]. Absorbed water was detected around 3500 cm^{-1} [37].

The FTIR analysis also shows that B-type carbonation (CO_3^{2-}signals at 1410, 1450, and 873 cm^{-1}) occurred during the Sr substituted calcium phosphate synthesis, although there is no carbonate source in the solution [34]. Such carbonation was due to the carbon dioxide in the reaction vessel, since the synthesis process was performed under normal atmosphere. The reactive absorption of atmospheric carbon dioxide by the solution occurred during the preparation of the solution [5].

The presence of the carbonate functional group during the fabrication of calcium phosphate nanoparticles via sol gel method has been reported in previous study [34]. Substitution of strontium ions in the apatite structure did not inhibit the carbonate substitution in the B-type carbonate position of the lattice. This simple sol gel method procedure under normal atmosphere results in the Sr and carbonate co-substituted calcium phosphate directly without using any carbonate source precursors. It has been reported previously that co-substitution of Sr and carbonate in a calcium phosphate lattice could enhance the biocompatibility properties and dissolution rate of nanoparticles [11, 34, 37].

The FTIR spectra of the Sr substituted samples show a decrease in the relative intensity of the absorption hydroxyl bands on increasing Sr. Furthermore, in agreement with Dahl et al. [21], and Alkhraisat et al. [38]. The hydroxyl stretching band progressively shifts to higher wave numbers with increasing the strontium content.

Substitution of strontium ions in apatite structure has no significant effect on the FTIR spectrum of calcium phosphate samples. Infrared spectra show the Sr and carbonate co-substitution in calcium phosphate lattice which is similar to the result of sol gel derived calcium phosphate nanoparticles [34]. Increasing the amount of Sr in the structure causes the shift of the hydroxyl band to higher wave numbers.

3.4 Specific surface area measurement

The values of the specific surface area (SSA) and average particle size (d_{BET}) of the samples are reported in Table 3.

Table 3 Specific surface area and d_{BET} values of Sr substituted samples

Sample	Sample composition	Specific surface area (m^2/g)	Equivalent spherical diameter, d_{BET} (nm)
1	0.0Sr-CaP	55	32
2	0.5Sr-CaP	62	31
3	1.0 Sr-CaP	74	27
4	5.0 Sr-CaP	91	18
5	10.0Sr-CaP	94	17

The specific surface area values determined through the BET method are consistent with the nano size particles i.e., in accordance with TEM results. A high specific surface area in the range of 50–90 m^2/g for Sr substituted calcium phosphate particles has been reported in other experiments [37, 38].

Table 3 shows that increasing the amount of strontium substitution in calcium phosphate structure results in nanoparticles with higher specific surface area. For a constant amount of calcium phosphate gene carrier, particles with higher values of specific surface area present more DNA binding sites at the surface [2–4]. Therefore, increasing the specific surface area of the calcium phosphate particles may enhance the DNA concentration in the final gene delivery complex,.and increase the amount of DNA in cytoplasm, that could improve the gene delivery efficiency.

BET analysis demonstrates that concentrations of strontium ions above 1% make nanoparticles with higher specific surface area and smaller particle size. This finding is in agreement with XRD and TEM results (Table 2 and Fig. 2), which show a higher amount of Sr substitution in calcium phosphate structure has a greater effect on the particle size of the products than the Sr concentration.

3.5 Zeta potential measurement

Cationic vectors with higher values of positive surface charge have better interaction with DNA and improve DNA condensation on the carrier, due to DNA's net negative charge [14, 15]. Zeta potential evaluation of Sr substituted nanoparticles has been performed at physiological pH (7.4). The results are shown in Table 4.

Although measuring the zeta potential of Sr substituted calcium phosphate in water medium shows net negative charge for the particles as reported previously [38]; the results of this study demonstrated that, measuring the zeta potential in physiological media results in positive surface charge which is more efficient for gene delivery applications.

Table 4 shows that increasing the amount of Sr concentration in the solution has no significant effect on the zeta potential of cationic substituted particles.

Table 4 Zeta potential measurement for Sr substituted calcium phosphate nanoparticles

Sample	Sample composition	Zeta potential (mV)
1	0.0Sr-CaP	4.5 ± 0.1
2	0.5Sr-CaP	5.0 ± 0.2
3	1.0 Sr-CaP	6.1 ± 0.1
4	5.0 Sr-CaP	7.3 ± 0.3
5	10.0Sr-CaP	7.8 ± 0.2

Accordingly, it could be concluded that the addition of Sr ions in calcium phosphate nanoparticles keeps the surface charge in the positive range in physiological medium, and makes positively charged nanoparticles. This could be an appropriate candidate for non viral gene delivery of negatively charged DNA parts to the cell surface.

3.6 Ion dissolution rate in simulated body fluid

Ca^{2+} and Sr^{2+} release of the calcium phosphate nanoparticles could be effective factor for endosomal escape of the gene delivery complex. Therefore, ion release regime of the Sr substituted calcium phosphate nanoparticles has been evaluated in simulated body fluid.

Figure 4 shows the diagram of the Ca^{2+} and Sr^{2+} release during two weeks of experiments with a two day interval. As expected, ion concentration of the SBF medium increased with respect to time. Sr and carbonate ions co-substitution in calcium phosphate lattice enhanced its dissolution rate. It was found that the calcium phosphate particles containing Sr exhibited a more abundant calcium release with respect to the Sr free HA powders.

Increasing the ion release from Sr containing particles has been reported before. Landi et al. [11] suggested the following sequence of powder solubility for the biological range of pH for different calcium phosphate: SrCHA > SrHA > HA. Where SrCHA is the Sr and carbonate co-substituted hydroxyapatite, SrHA is Sr substituted hydroxyapatite and HA is Sr and carbonate free hydroxyapatite. A higher dissolution rate for Sr and carbonate co-substituted calcium phosphate nanoparticles was also reported by Boanini et al. [18].

The results of ion release measurements are completely in agreement with Pan et al. work which confirmed that, the solubility of Sr substituted hydroxyapatite significantly and steadily increases with the increase of strontium content [12].

Substitution of Sr in apatite structure decreases the crystallinity and crystal size of the nanoparticles (Table 2) which causes the higher dissolution rate. On the other hand, it has been suggested that the Sr destabilizes the apatite structure [12]. Destabilization of crystal structure occurred

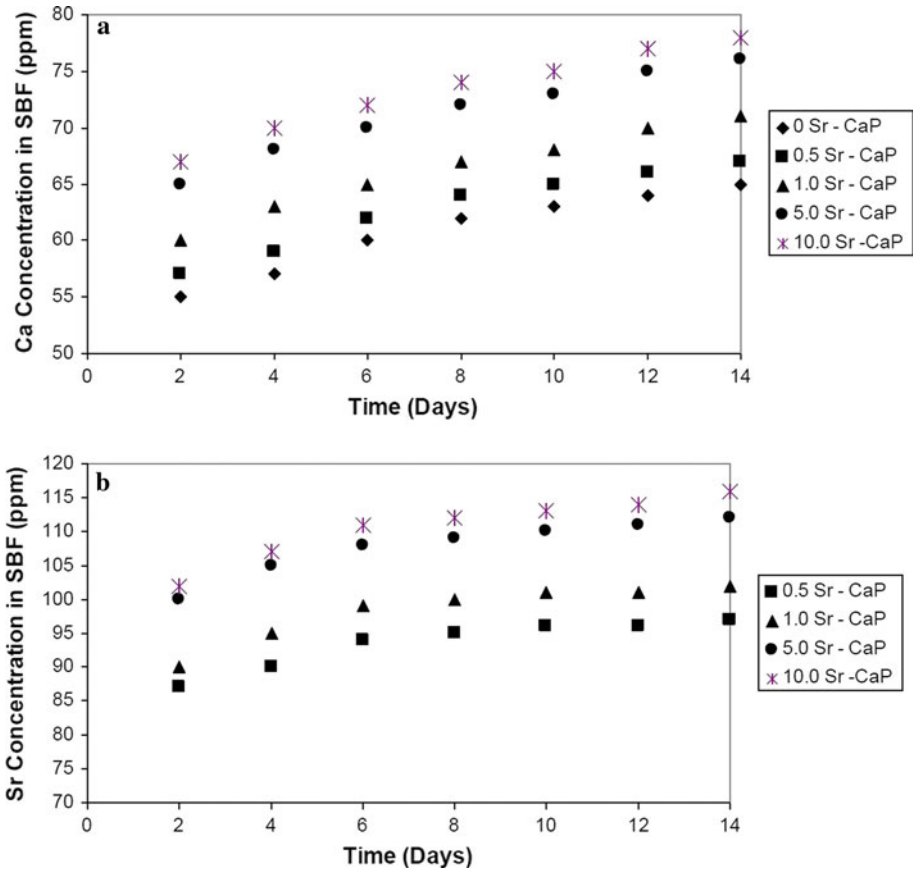

Fig. 4 (**a**) Ca^{2+} and (**b**) Sr^{2+} ions release in simulated body fluid

because larger strontium atoms were substituted for calcium ions in a calcium phosphate lattice [18].

The present results are in agreement with Kannan et al. [10], and Christoffersen et al. [19], indicate that the solubility of strontium substituted apatite increases with the increasing strontium content.

The result of the dissolution rate evaluation shows higher amounts of Ca^{2+} and Sr^{2+} release for Sr substituted calcium phosphate nanoparticles in comparison with Sr free particles.

This study shows that smaller the particle size, lower the crystallinity and higher dissolution rates of the Sr substituted calcium phosphate nanoparticles could potentially increase the efficiency of these novel non viral vectors in gene delivery applications.

4 Conclusions

Strontium substituted calcium phosphate nanoparticles were prepared using a simple sol gel method. The incorporation of Sr in apatite structure was proved by increased lattice parameters of the samples in comparison to the Sr free calcium phosphate. Increasing the concentration of Sr ions in solution, decreased the particle size and crystallinity of the samples but did not have a significant effect on phase composition.

The simple sol gel method used in this study resulted in Sr substituted calcium phosphate nanoparticles with nano size structure, high specific surface area, a positively charged surface, and a high dissolution rate.

These improved properties could potentially increase the gene delivery efficiency using this novel non viral gene delivery vectors by increasing the DNA condensation and concentration on the carrier as well as increasing the endosomal escape of the gene-vector complex.

References

1. Phillips JE, Gersbach, Garcıa AJ. Virus-based gene therapy strategies for bone regeneration. Biomaterials. 2007;28:211–29.
2. Kofron MD, Laurencin CT. Bone tissue engineering by gene delivery. Adv Drug Deliv Rev. 2006;58:555–76.
3. Fu H, Hu Y, McNelis T, Hollinger JO. A calcium phosphate-based gene delivery system. J Biomed Mater Res A. 2005; 74:40–8. doi: 10.1002/jbm.a.30267.
4. Olton D, Li J, Wilson ME, Rogers T, Close J, Huang L, Kumta PN, Sfeir C. Nanostructured calcium phosphates (NanoCaPs) for non-viral gene delivery: influence of the synthesis parameters on transfection efficiency. Biomaterials. 2007;28:1267–79.

5. Li ZY, Lam WM, Yang C, Xu B, Ni GX, Abbah SA, Cheung KMC, Luk KDK, Lu WW. Chemical composition, crystal size and lattice structural changes after incorporation of strontium into biomimetic apatite. Biomaterials. 2007;28:1452–60.
6. Alkhraisat MH, Rueda C, Cabrejos-Azama J, Lucas-Aparicio J, Marino FT, Garcia-Denche JT, Jerez LB, Gbureck U, Cabarcos EL. Loading and release of doxycycline hyclate from strontium-substituted calcium phosphate cement. Acta Biomater. 2010;6:1522–8. doi:10.1016/j.actbio.2009.10.043.
7. Qi G, Zhang S, Khor KA, Weng W, Zeng X, Liu C. An interfacial study of sol–gel-derived magnesium apatite coatings on Ti6Al4 V substrates. Thin Solid Films. 2008;516:5172–5.
8. Pina S, Torres PM, Goetz-Neunhoeffer F, Neubauer J, Ferreira JMF. Newly developed Sr-substituted a-TCP bone cements. Acta Biomater. 2010;6(3):928–35.
9. Schoenberg HP. Extent of strontium substitution for calcium in hydroxyapatite. Biochem Biophys Acta. 1963;75:96–103.
10. Kannan S, Goetz-Neunhoeffer F, Neubauer J, Pina S, Torres PMC, Ferreira JMF. Synthesis and structural characterization of strontium- and magnesium-co-substituted b-tricalcium phosphate. Acta Biomater. 2010;6:571–6.
11. Landi E, Sprio S, Sandri M, Celotti G, Tampieri A. Development of Sr and CO_3 co-substituted hydroxyapatites for biomedical applications. Acta Biomater. 2008;4:656–63.
12. Pan HB, Li ZY, Lam WM, Wong JC, Darvell BW, Luk KDK, Lu WW. Solubility of strontium-substituted apatite by solid titration. Acta Biomater. 2009;5:1678–85.
13. Lam WM, Pan HB, Li ZY, Yang C, Chan WK, Wong CT, Luk KDK, Lu WW. Strontium-substituted calcium phosphates prepared by hydrothermal method under linoleic acid–ethanol solution. Ceram Int. 2010;36:683–8.
14. Wen-Yih C, Ming-Shen L, Po-Hsun L, Pei-Shun T, Yung C, Shuichi Y. Studies of the interaction mechanism between single strand and double-strand DNA with hydroxyapatite by microcalorimetry and isotherm measurements. Colloids Surf. A. 2007;295(1–3):274–83.
15. Gerstein AS. Molecular biology problem solver: a laboratory guide. Newyork: Wiley-IEEE; 2001.
16. Boussif O, Lezoualc'h F, Zanta MA, Mergny MD, Scherman D, Demeneix B, Behr JP. A versatile vector for gene and oligonucleotide transfer into cells in culture and in vivo: polyethylenimine. Proc Natl Acad Sci USA. 1995;92:7297–301.
17. Taira K, Kataoka K, Niidome T. Non-viral gene therapy—gene design and delivery. Tokyo: Springer-Verlag; 2005.
18. Boanini E, Gazzano M, Bigi A. Ionic substitutions in calcium phosphates synthesized at low temperature. Acta Biomater. 2009;6:1882–4. doi: 10.1016/j.actbio.2009.12.041.
19. Christoffersen J, Christoffersen MR, Kolthoff N, Brenholdt O. Effects of strontium ions on growth and dissolution of hydroxyapatite, and on bone mineral detection. Bone. 1997;20(1):47–54.
20. Maitra A. Calcium phosphate nanoparticles: second-generation nonviral vectors in gene therapy. Expert Rev Mol Diagn. 2005;5(6):893–905.
21. Dahl SG, Allain P, Marie PJ, Mauras Y, Boivin G, Ammann P, Tsouderos Y, Delmas PD, Christiansen C. Incorporation and distribution of strontium in bone. Bone. 2001;28(4):446–53.
22. Bracci B, Torricelli P, Panzavolta S, Boanini E, Giardino R, Bigi A. Effect of Mg^{2+}, Sr^{2+}, and Mn^{2+} on the chemico-physical and in vitro biological properties of calcium phosphate biomimetic coatings. J Inorg Biochem. 2009;103:1666–74.
23. Marie PJ, Ammann P, Boivin G, Rey C. Mechanisms of action and therapeutic potential of strontium in bone. Calcif Tissue Int. 2001;69:121–9.
24. Cazalbou S, Combes C, Rey C. Biomimetic approach for strontium containing Ca–P bioceramics with enhanced biological activity. Key Eng Mater. 2001;192–195:147–50.
25. Verberckmoes SC, Behets GJ, Oste L, Bervoets AR, Lamberts LV, Drakopoulos M, et al. Effects of strontium on the physicochemical characteristics of hydroxyapatite. Calcif Tissue Int. 2004;75:405–15.
26. Li YW, Leong JCY, Lu WW, Luk KDK, Cheung KMC, Chiu KY, et al. A novel injectable bioactive bone cement for spinal surgery: a developmental and preclinical study. J Biomed Mater Res. 2000;52:164–70.
27. Fathi MH, Hanifi A. Evaluation and characterization of nanostructure hydroxyapatite powder prepared by solgel method. J Mater Lett. 2007;61(18):3978–83.
28. Fathi MH, Hanifi A. Sol–gel derived nanostructure hydroxyapatite powder and coating: aging time optimization. Adv Appl Ceram. 2009;108(6):363–8.
29. Chung RJ, Hsieh MF, Huang KC, Chou FI, Perng LH. Preparation of porous HA/beta-TCP biphasicbioceramic using a molten salt process. Key Eng Mater. 2006;309–311:1075–8.
30. Patterson AL. The Scherrer formula for X-ray particle size determination. Phys Rev. 1939;56:978.
31. Landi E, Tampieri A, Celotti G, Sprio S. Densification behavior and mechanisms of synthetic hydroxyapatites. J Eur Ceram Soc. 2000;20:2377–87.
32. Cacciotti I, Bianco A, Lombardi M, Montanaro L. Mg-substituted hydroxyapatite nanopowders: synthesis, thermal stability and sintering behaviour. J Eur Ceram Soc 2009;29:2969–78.
33. Ren F, Xin R, Ge X, Leng Y. Characterization and structural analysis of zinc-substituted hydroxyapatites. Acta Biomater. 2009;5:3141–9.
34. Fathi MH, Hanifi A, Mortazavi V. Preparation and bioactivity evaluation of bone-like hydroxyapatite nanopowder. J Mater Process Technol. 2008;202:536–42.
35. Renaudin G, Laquerriere P, Filinchuk Y, Jallotd E, Nedelec JM. Structural characterization of sol–gel derived Sr-substituted calcium phosphates with anti-osteoporotic and anti-inflammatory properties. J Mater Chem. 2008;18:3593–600.
36. Bigi A, Boanini E, Capuccini C, Gazzano M. Strontium-substituted hydroxyapatite nanocrystals. Inorg Chim Acta. 2007;360:1009–16.
37. Landi E, Tampieri A, Mattioli-Belmonte M, Celotti G, Sandri M, Gigante A, Fava P, Biagini G. Biomimetic Mg- and Mg,CO_3-substituted hydroxyapatites: synthesis characterization and in vitro behaviour. J Eur Ceram Soc. 2006;26:2593–601.
38. Alkhraisat MH, Moseke C, Blanco L, Barralet JE, Lopez-Carbacos E, Gbureck U. Strontium modified biocements with zero order release kinetics. Biomaterials. 2008;29:4691–7.